Nanomagnetics

Laser-Reduced Zeolite Imidazole Framework-67 as Magnetic Absorbents for Oil Separation in Water

Junfeng Huang[1], Kam Chuen Yung[1], Guijun Li[1], Zhuoxun Wei[2], and Zhengong Meng[2]

[1] Department of Industrial and Systems Engineering, The Hong Kong Polytechnic University, Hong Kong
[2] College of Chemistry and Environmental Engineering, Shenzhen University, Shenzhen 518060, China

Received 30 Nov 2018, revised 21 Dec 2018, accepted 1 Jan 2019, published 14 Jan 2019, current version 6 Feb 2019.

Abstract—We reduced zeolite imidazole framework-67 by laser so as to prepare porous carbon materials embedded with cobalt nanoparticles. The composites exhibited ferromagnetic behavior. The parameters of laser reduction were optimized for oil absorption with high capacity and good reusability. This approach can open a new class of ferromagnetic porous absorbents and represent advancement toward overcoming the limitations of oil absorption.

Index Terms—Nanomagnetics, ZIF-67, laser reduction, ferromagnetic, oil absorption.

I. Introduction

The rapid increase of fossil fuel usage in industrial and social development is inescapable. However, oil spillages caused during production and transportation have led to severe environmental issues and ecological damage. Various materials have been studied for collecting leaking oil, including graphene aerogels [Xu 2015], silylated nanocellulose sponges [Lu 2017], polyurethane sponges [Tran 2017], and poly(styrene-divinylbenzene) foam [Zhang 2015]. Porous hydrophobic polymers are the major oil absorption carriers, but their irregular pore size, low porosity, and poor thermal stability still restrict their capacity for oil absorption. Metal–organic frameworks (**MOF**s) have attracted a lot of attention due to their high porosity [Wu 2017], which made them suitable for physical absorption. Meanwhile, structure stability of MOFs in high temperature also makes them competitive, as compared with polymer carriers. Inserted magnetic particles are easily separated from polymers under heat, while the carbon framework of MOFs makes the structure stable [Meng 2018]. Conjugation of the merits of MOFs and their applications in a magnetic field has gained them high popularity and increasing interest [Kurmoo 2009]. However, ferromagnetic MOFs were still rare, and the existing ones revealed small coercivity [Dong 2018]. Zeolitic imidazolate framework (**ZIF**), as one of the important subclass of MOFs, was also studied widely. ZIF-67 was selected as the initial material, due to its great porosity and chemical and thermal stability [Shi 2011].

To date, the modification of materials via laser reduction has been massively explored in recent years [El-Kady 2012]. Low cost, easy control, and time saving have made laser reduction an important contributor in scientific development. However, research on laser modification for MOFs has not been broadly explored.

Herein, laser power was used to reduce ZIF-67 into ferromagnetic porous carbon materials. The resultant Co-embedded composites also retained the high porosity and big surface area. The effect of laser writing speed and hatch space on materials' properties and structure was fully studied. The morphology, crystalline structure, and magnetic properties of ZIF-67 and laser-reduced ZIF-67 (**LR-ZIF-67**) were also measured.

Table 1. List of samples with different parameters and their element content.

Sample		ZIF-67	A	B	C	D	E
Hatch space (μm)		N/A	60	60	60	40	10
Writing speed (mm/min)		N/A	1500	1200	1000	1000	1000
Cobalt (%)	W	34.35	33.69	36.98	40.19	28	51.36
	A	9.64	9.38	11.07	12.5	7.59	18.65
Carbon (%)	W	65.65	66.31	53.23	48.81	61.72	36.69
	A	90.36	90.62	78.14	74.8	82.17	65.36
Oxygen (%)	W	N/A	N/A	9.79	11	10.25	11.95
	A			10.79	12.65	10.24	15.99

II. EXPERIMENT

ZIF-67 was prepared according to the literature method. In brief, $CoCl_2.6H_2O$ and 2-methylimidazole were dissolved in methanol to form solutions 1 and 2, respectively, and then solutions 1 and 2 were mixed together. The mixture was aged overnight at room temperature to obtain purple precipitation, and the precipitates were collected by centrifugal separation. The as-synthesized ZIF-67 was dispersed in ethanol and then dropped on a silicon wafer, premodification by laser was done after drying on the hotplate at 50 °C.

A simple laser writing system was used for laser reduction [Yung 2016a]. Briefly, a 405 nm GaN laser head with 0.4 W was installed on a tailor-made X-Y moving system, and the writing system was controlled by computer. Particles were reduced by laser at different writing speed and hatch space, as listed in Table 1. Acetic acid was used to etch the residual ZIF-67 particles. Reduced samples were washed by water and ethanol, and then oven-dried at 100 °C.

Corresponding author: Zhengong Meng (e-mail: mengzg@szu.edu.cn).
Digital Object Identifier 10.1109/LMAG.2019.2892930

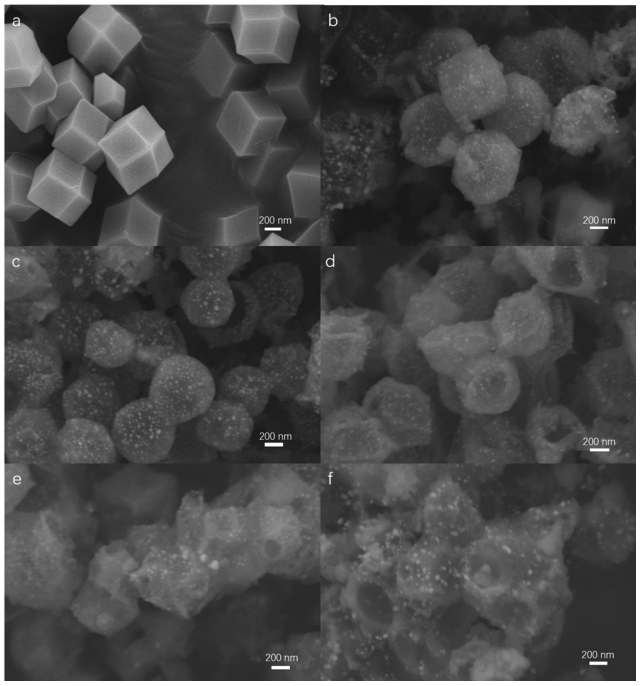

Fig. 1. SEM image of (a) synthesized ZIF-67 and (b)–(f) samples A to E.

The oil adsorption capacities of samples were calculated by using weight measurements, which can be expressed as

$$C_a\,(\mathrm{g/g}) = (W_a - W_b)\,/\,W_c \tag{1}$$

where W_a and W_b are the weight of the dish of water with oil in the initial state and after oil absorption and particles removal, respectively, and W_c is the mass of particles.

The crystal structures were identified by X-ray diffraction (**XRD**) with Cu K radiation. The morphology and composition were studied by scanning electronic microscope (**SEM**) and energy-dispersive X-ray spectroscopy. For measuring magnetic properties, a vibrating-sample magnetometer was used to measure the magnetic hysteresis loop.

III. RESULTS AND DISCUSSION

The morphology and microstructure of ZIF-67 and LR-ZIF-67 were measured by SEM (see Fig. 1). ZIF-67 with regular dodecahedral shape after laser modification resulted in a changed particle surface and partially deformed particle shape. The tremendous energy from the laser would damage the chemical bonds in the organic frameworks, and thereby plenty of metal cores were exposed on the particles' surface. It is comprised of laser irradiation and thermal effect. Laser irradiation provides massive energy to break down bonds between cobalt and organic ligand [Yung 2016b]. The required energy is called bond dissociation energy. Besides, the laser also brings heat on ZIF-67 and carbonizes it, and cobalt particles are decomposed and deposited into carbon metrics [Torad 2014]. Furthermore, the reduced samples presented strong structural stability after laser reduction, and cavities began to form during the laser writing process. Since it is physical absorption for LR-ZIF-67, the larger pore size and cavity volume of materials with larger porosity can exhibit larger absorption ability [Zhong 2018]. As

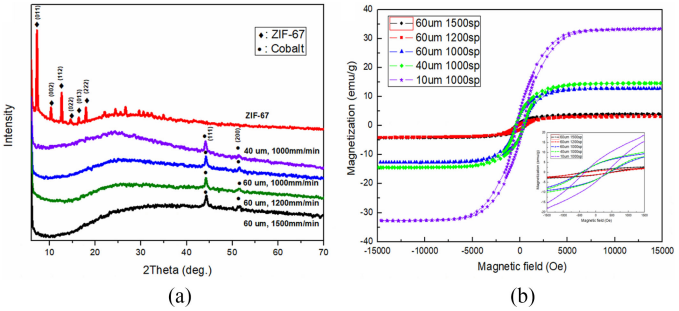

(a) (b)

Fig. 2. (a) XRD patterns of ZIF-67 and LR-ZIF-67. (b) Hysteresis loop of LR-ZIF-67.

writing speed decreased, samples began to deform heavily, but they still maintained clear polyhedral structure [see Fig. 1(c) and (d)]. When the spot size of the laser was 60 μm in diameter, ZIF-67 was only once reduced by laser, which would prevent deep oxidation inside the particles' core; hence, reaction with oxygen only occurred on the surface. However, the hatch space was set lower than 60 μm, and the samples were reduced more than once. So the surrounding oxygen became easier for the inner part of the particles and changed their structure. Table 1 lists the elemental content for each of the samples. Due to the low concentration of oxygen in ZIF-67, the signal of oxygen was not detected, as well as for sample A. Fast laser writing without repetitive reduction only mildly modified ZIF-67. The change of writing speed and hatch space resulted in the difference of energy transferred by laser, which affected the level of carbonization. The gasification of carbon by reaction with oxygen for forming carbon dioxide led to the decrease of the content of carbon and thereby the increase of the content of cobalt and oxygen. A decrease in writing speed enlarged retention time and generated more energy to disconnect the metal and organic bond, and then decreased the carbon content. The separation of organic bond also led to the emergence of the cavity, and these cavities thereby provided paths to carry oxygen.

To identify the crystal structure, XRD in Fig. 2(a) was used to measure ZIF-67 and LR-ZIF-67. The pattern shows a typical ZIF-67 crystal with distinct peak signal (011), (112), and other major peaks. Modification in ZIF-67 by laser caused a completely changed crystal structure. LR-ZIF-67 was entirely transformed into cobalt. It demonstrated that the laser destroyed the link between cobalt and the organic bond, and the decomposed cobalt atom bared on top of the framework exhibited a strong crystalline signal. LR-ZIF-67 with 60 μm hatch space exhibited a clear signal of (200) phase. The change in laser writing speed did not have a significant impact in the deformation of crystalline structure. In contrast, when hatch space decreased to 40 μm, the signal of (200) phase in LR-ZIF-67 hid in background noise. The crystal structure was destroyed by laser through multiple heating.

The hysteresis loop of samples was also measured in Fig 2(b), and the coercivities of samples A, B, and C were 433.16, 410.91, and 436.13 Oe, respectively. However, there was no obvious alteration owing to the weak effect of writing speed. The saturation magnetization of LR-ZIF-67 also revealed similar condition. However, the magnetization of sample C (12.78 emu/g) exhibited an increase as compared to samples A (3.93 emu/g) and B (3.38 emu/g); it demonstrated that slower laser writing speed (1000 mm/min) strongly

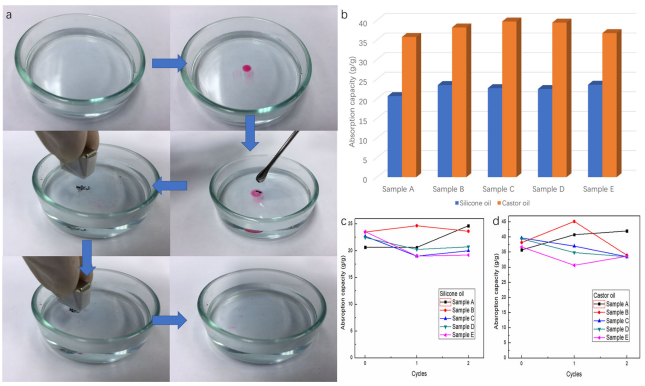

Fig. 3. (a) Schematic diagram of oil absorption. (b) Oil absorption capacity of different samples for silicone oil and castor oil. (c) and (d) Reusability of different samples in silicone oil and castor oil, respectively.

increased the induced magnetic dipole moments. In contrast, hatch space for laser reduction in samples exhibited distinct effects on magnetic behaviors. Coercivity decreased and saturation magnetization increased as hatch space was reduced. Coercivities of samples D and E were 410.91 and 329.32 Oe, respectively. A clear drop trend was also presented. In contrast, magnetization increased to 33.35 emu/g when the hatch space was dropped to 10 μm owing to the increase of the generation of magnetic domains inside cobalt. The increase of the composition of the magnetic phase caused by the increase of cobalt generated a stronger exchange in coupling interaction, and thereby led to an increase in remanent magnetization [Xu 2018]. Meanwhile, the increase in the extent of crystallization and density of domains also contributed to the increase in magnetization [Liu 2010]. Sample E exhibited the largest saturation magnetization, since magnetic domains did not hide during reformation.

Castor oil and silicone oil were selected for oil absorption. Oil was dyed with iron oxide pigments in red for distinct observation. The process of oil absorption and recycling for samples is shown in Fig. 3(a). The oil was poured into water as an oil spill, and then samples were added to absorb the spilled oil; after the absorption completed, a magnet was used to remove oil-absorbed samples. Recycled samples were then washed using ethanol and water with ultrasonic to eliminate absorbed oil. Collected samples were dried at 65 °C for 6 h. Oil absorption capacity of samples is shown in Fig. 3(b) and indicated that oil absorption capacity of castor oil is much greater than that of silicone oil. On average, the absorption capacity of castor oil can reach up to 37.96 g/g, whereas that of silicone oil only reaches 22.58 g/g. Sample B showed strongest oil absorption ability for silicone oil, whereas sample C exhibited best absorption with castor oil. Slower laser writing speed on samples exhibited relatively high oil absorption ability. Fig. 3(c) and (d) represented reusability of samples for oil absorption for silicone oil and castor oil, respectively. Even after thermal decomposition and carbonization, the structure of LR-ZIF-67 still exhibited relatively regular shape, although the particle surface was distorted. Due to the thermal stability of MOFs materials, repeatability of oil absorption can be guaranteed. Sample A demonstrated better absorption ability after recycling for oil absorption for both oils. However, after recycling for a second time, oil absorption ability started to weaken. It was because the deformations of samples' structure caused by the decrease of writing speed and hatch speed resulting in the decrease of cavity volume and thereby reduce the absorption ability.

IV. CONCLUSION

Ferromagnetic porous carbon materials were prepared successfully by laser reduction of ZIF-67 with different hatch space and writing speed. The morphology of the resultant materials was maintained roughly while cobalt nanoparticles were embedded. LR-ZIF-67 in 60 μm hatch space and 1200 and 1000 mm/min showed optimum oil absorption capacity for silicone oil and castor oil, but LR-ZIF-67 in 1500 writing speed exhibited optimum reusability after recycling.

ACKNOWLEDGMENT

This work was supported in part by a grant from the Research Committee of The Hong Kong Polytechnic University under student account code RUV2 and in part by the National Natural Science Foundation of China under Grant 21701112.

REFERENCES

Dong R, Zhang Z, Tranca D C, Zhou S, Wang M, Adler P, Liao Z, Liu F, Sun Y, Shi W, Zhang Z, Zschech E, Mannsfeld S C B, Felser C, Feng X (2018), "A coronene-based semiconducting two-dimensional metal-organic framework with ferromagnetic behavior," *Nature Commun.*, vol. 9, 2637, doi: 10.1038/s41467-018-05141-4.

El-Kady M F, Strong V, Dubin S, Kaner R B (2012), "Laser scribing of high-performance and flexible graphene-based electrochemical capacitors," *Science*, vol. 335, pp. 1326–1330, doi: 10.1126/science.1216744.

Kurmoo M (2009), "Magnetic metal–organic frameworks," *Chem. Soc. Rev.*, vol. 38, pp. 1353–1379, doi: 10.1039/B804757J.

Ming-Quan L, Xiang-Qian S, Xian-Feng M, Song F, Jun X (2010), "Fabrication and magnetic property of M-type strontium ferrite nanofibers by electrospinning," *J. Inorg. Mater.*, vol. 25, pp. 68–72, doi: 10.3724/Sp.J.1077.2010.00068.

Lu Y, Wang Y, Liu L, Yuan W (2017), "Environmental-friendly and magnetic/silanized ethyl cellulose sponges as effective and recyclable oil-absorption materials," *Carbohydrate Polym.*, vol. 173, pp. 422–430, doi: 10.1016/j.carbpol.2017.06.009.

Meng Z, Ho C-L, Wong H-F, Yu Z-Q, Zhu N, Li G, Leung C-W, Wong W-Y (2018), "Lithographic patterning of ferromagnetic FePt nanoparticles from a single-source bimetallic precursor containing hemiphasmidic structure for magnetic data recording media," *Sci. China Mater.*, to be published, doi: 10.1007/s40843-018-9350-4.

Shi Q, Chen Z, Song Z, Li J, Dong J (2011), "Synthesis of ZIF-8 and ZIF-67 by steam-assisted conversion and an investigation of their tribological behaviors," *Angew. Chemie*, vol. 123, pp. 698–701, doi: 10.1002/anie.201004937.

Torad N L, Hu M, Ishihara S, Sukegawa H, Belik A A, Imura M, Ariga K, Sakka Y, Yamauchi Y (2014), "Direct synthesis of MOF-derived nanoporous carbon with magnetic Co nanoparticles toward efficient water treatment," *Small*, vol. 10, pp. 2096–2107, doi: 10.1002/smll.201302910.

Tran V-H T, Lee B-K (2017), "Novel fabrication of a robust superhydrophobic PU@ZnO@Fe_3O_4@SA sponge and its application in oil-water separations," *Sci. Rep.*, vol. 7, 17520, doi: 10.1038/s41598-017-17761-9.

Wu M-X, Yang Y-W (2017), "Metal–organic framework (MOF)-based drug/cargo delivery and cancer therapy," *Adv. Mater.*, vol. 29, 1606134, doi: 10.1002/adma.201606134.

Xu S, Wang Z, Su R, Han N, Xie A, Wang L, Li H (2018), "Structure and magnetic properties of multi-morphological $CoFe_2O_4$/CoFe nanocomposites by one-step hydrothermal synthesis," *Ceram Int.*, vol. 44, pp. 9377–9383, doi: 10.1016/j.ceramint.2018.02.152.

Xu X, Li H, Zhang Q, Hu H, Zhao Z, Li J, Li J, Qiao Y, Gogotsi Y (2015), "Self-sensing, ultra light, and conductive 3D graphene/iron oxide aerogel elastomer deformable in a magnetic field," *ACS Nano*, vol. 9, pp. 3969–3977, doi: 10.1021/nn507426u.

Yung W K C, Sun B, Huang J, Jin Y, Meng Z, Choy H S, Cai Z, Li G, Ho C L, Yang J, Wong W Y (2016a), "Photochemical copper coating on 3D printed thermoplastics," *Sci. Rep.*, vol. 6, 31188, doi: 10.1038/srep31188.

Yung W K C, Sun B, Meng Z, Huang J, Jin Y, Choy H S, Cai Z, Li G, Ho C L, Yang J, Wong Y W (2016b), "Additive and photochemical manufacturing of copper," *Sci. Rep.*, vol. 6, 39584, doi: 10.1038/srep39584.

Zhang N, Jiang W, Wang T, Gu J, Zhong S, Zhou S, Xie T, Fu J (2015), "Facile preparation of magnetic poly(styrene-divinylbenzene) foam and its application as an oil absorbent," *Ind. Eng. Chem. Res.*, vol. 54, pp. 11033–11039, doi: 10.1021/acs.iecr.5b01847.

Zhong G, Liu D, Zhang J (2018), "The application of ZIF-67 and its derivatives: Adsorption, separation, electrochemistry and catalysts," *J. Mater. Chem. A*, vol. 6, pp. 1887–1899, doi: 10.1039/C7TA08268A.